

# 1 A CRISPR/Cas12a-assisted platform for identification 2 and quantification of single CpG methylation sites

3 J.E. van Dongen<sup>1</sup>; J.T.W. Berendsen<sup>1</sup>; J.C.T. Eijkel<sup>1</sup>; L.I. Segerink<sup>1</sup>

4 BIOS Lab on a Chip group, MESA+ Institute for Nanotechnology, Technical Medical Centre, Max Planck Institute  
5 for Complex Fluid Dynamics, University of Twente, Enschede, the Netherlands  
6

7 **Clustered Regularly Interspaced Short Palindromic Repeats (CRISPR)/associated nuclease (Cas)**  
8 **systems have repeatedly shown to have excellent performance in nucleotide sensing applications<sup>1–</sup>**  
9 **<sup>5</sup>. High specificity and selectivity of Cas effector proteins is determined by the CRISPR RNA's (crRNA's)**  
10 **interchangeable spacer sequence, as well as position and number of mismatches between target**  
11 **sequence and the crRNA sequence<sup>1</sup>. Some diseases are characterized by epigenetic alterations**  
12 **rather than nucleotide changes, and are therefore unsuitable for CRISPR-assisted sensing methods.**  
13 **Here we demonstrate a method to discriminate single CpG site methylation in DNA, which is an**  
14 **epigenetic alteration, by the use of methylation-sensitive restriction enzymes (MSREs) followed by**  
15 **Cas12a-assisted sensing. Non-methylated sequences are digested by MSREs, resulting in**  
16 **fragmentation of the target sequence that influences the R-loop formation between crRNA and**  
17 **target DNA. We show that fragment size, fragmentation position and number of fragments influence**  
18 **the subsequent collateral *trans*-cleavage activity towards single stranded DNA (ssDNA), enabling**  
19 **deducting the methylation position from the cleavage activity. Utilizing MSREs in combination with**  
20 **Cas12a, single CpG site methylation levels of a cancer gene were for the first time determined. The**  
21 **modularity of both Cas12a and MSREs provide a high level of versatility to the Cas12a–MSRE**  
22 **combined sensing method, which opens the possibility to easily and rapidly study single CpG**  
23 **methylation sites for disease detection.**  
24

25 CRISPR/Cas systems have revolutionized biotechnology and synthetic biology<sup>6–9</sup>. Of special interest for  
26 the sensor field are the type V and VI effector proteins, two subclasses of the class 2 Cas proteins.  
27 These proteins showcase, besides targeted *cis*-cleavage, untargeted *trans*-cleavage activity. This *trans*-  
28 cleavage activity has multiple turnovers, enabling a signal amplification of up to 10,000<sup>5</sup>, which can be  
29 deployed in sensor applications to lower the limit of detection.  
30

31 For double stranded DNA (dsDNA) sensing, type V effector protein Cas12a is mostly used. Critical for  
32 both *trans*- and *cis*-cleavage activities of Cas12a is the R-loop formation step, where the crRNA and  
33 target strand of the dsDNA hybridize and the catalytic site is revealed (Extended Data Fig. 1). Due to  
34 the late transition state for R-loop formation, Cas12a is generally able to discriminate against  
35 mismatches across the R-loop, determining its low mismatch tolerance<sup>10</sup>. However, the degree of  
36 mismatch tolerance greatly depends on the origin of the effector protein and the position of the  
37 mismatch<sup>1</sup>. The nucleotides in the so-called 'seed' region hybridize with the target protospacer  
38 adjacent motif (PAM) proximal nucleotides and are considered critical in target affinity<sup>11</sup>, and  
39 mismatches in this region strongly negatively affect the *trans*-cleavage activity. PAM-distal mismatches  
40 show a much lower effect on the *trans*-cleavage activity, and only 15 out of 23 PAM-proximal matching  
41 nucleotides are needed for (temporary) binding of (enzymatically deactivated) Cas12a<sup>12</sup>.  
42

43 While many diseases could be related to single changes in the DNA nucleotides, not all genetic  
44 modifications related to diseases include changes in nucleotide sequences. In the last decade, cancer  
45 biomarker research has focused on biomarkers representing epigenetic alterations associated with the  
46 development of cancer<sup>13</sup>. One of these epigenetic events includes DNA (hyper)methylation.  
47 Methylated cytosines in CpG dinucleotides are an epigenetic alteration to the DNA, that is involved in  
48 both healthy processes like embryogenic development and transcriptional regulation, as well as in less  
49 benign processes such as autoimmune diseases and several cancer types<sup>14–16</sup>. These alterations can  
50 generally not be differentiated by Cas12 as a mismatch and are therefore, in principle, unsuitable for  
51 CRISPR sensing methods. Li *et al.* bypassed this issue by combining their HOLMESV2 with bisulfite  
52 conversion. However, bisulfite-based techniques are time consuming and labor-intensive chemical

53 treatments that damage DNA, induce (unwanted) DNA fragmentation, have limited throughput, and  
54 dramatically reduce the genome complexity, making specific targeting of sequences more difficult<sup>17</sup>.  
55 An alternative method to bisulfite conversion is the use of MSREs. Conventionally, MSREs are  
56 combined with quantitative polymerase chain reaction (qPCR) amplification for quantification  
57 purposes. However, this comes with several drawbacks: qPCR requires relatively long amplicon lengths  
58 (70-200 bp), and these amplicons should contain at least two MSRE restriction sites to reliably inhibit  
59 amplification for non-methylated samples<sup>18</sup>. Therefore, it is not possible to investigate the methylation  
60 levels of single CpG dinucleotides, which has been shown to be strongly associated with the  
61 development of gastric, liver and colon cancers<sup>19,20</sup>.

62  
63 A method to bypass both the long amplicon length and the need of multiple restriction sites to visualize  
64 the methylation level could be MSRE-based CRISPR/Cas sensing. In this case of restriction by MSREs  
65 prior to addition of the Cas effector protein, the fragmentation would affect the R-loop formation,  
66 thereby slowing down the *trans*-cleavage activity.

67  
68 **Shorter target fragments decrease, and longer target fragments increase *trans*-cleavage activity**  
69 When combining MSREs with Cas12a, the R-loop formation between the crRNA and non-methylated  
70 target DNA strands will be disrupted. To our knowledge the effect of the resulting short(er) target  
71 fragments complementary to crRNA was only previously touched upon by Chen *et al.*, who showed  
72 that target strand cleavage by Cas12a is not required to trigger the non-specific collateral cleavage  
73 activity towards ssDNA, but decreases the amount of *trans*-cleavage activity dramatically<sup>1</sup>. From  
74 previous work by Swarts and Jinek<sup>21</sup> and Chen *et al.*<sup>1</sup> we hypothesize that the most important  
75 prerequisite for *trans*-cleavage is the structural rearrangement of Cas12a to reveal the RuvC catalytic  
76 site by the R-loop formation, followed by clearance (See Supplementary information, section 1). This  
77 clearance can result either from *cis*-cleavage of target strands followed by diffusion of the PAM-distal  
78 fragment, or is not needed, due to the binding of short(er) target strands that do not interfere with  
79 the RuvC catalytic site. Therefore, we expect a tradeoff between R-loop formation length and clearance  
80 of the RuvC catalytic site.

81  
82 To experimentally quantify the effect of different target sequence lengths on Cas12a *trans*-cleavage,  
83 we tested the ability of synthetic oligonucleotides of different lengths to activate the *trans*-cleavage  
84 activity of Cas12a. Different target sequences were added to Cas12a and *trans*-cleavage was followed  
85 resulting in an increase in fluorescence by addition of a reporter DNA, which contained a fluorophore-  
86 quencher pair. To see whether the GC-content of the target sequences influenced the activity, we  
87 selected the MAL gene with a high GC-content, for which it is known that its methylation is related to  
88 several cancer types<sup>22-26</sup>, and a randomly designed sequence with a low GC-content (Extended Data  
89 Fig. 2). Besides the GC-content, the spacer length of the crRNA was varied as well, as it is known from  
90 literature that this length could strongly affect the cleavage efficiency of Cas12a<sup>27,28</sup>. Figure 1a and 1b  
91 show the results of different target fragment lengths of the high GC-content MAL gene at different  
92 concentrations (for 0.1 nM see Extended Data Fig. 3). Independent of the GC-content or crRNA length,  
93 the highest *trans*-cleavage activity could be observed for fragments from 15 bp match to the crRNA  
94 and onwards, which is in agreement with the length of PAM-distal mismatches that are accepted for  
95 enzymatically deactivated Cas12a binding<sup>12</sup>. Remarkably, the highest *trans*-cleavage activity of Cas12a  
96 is not observed for a DNA fragment that spans the total crRNA length, but for shorter fragments. This  
97 could be explained by a conserved aromatic residue (W382) of Cas12a that stacks on position 20 of the  
98 crRNA, preventing further R-loop propagation of the RNA:DNA duplex<sup>10,29-31</sup> and causing bases on  
99 position 20 and onwards to not further contribute to revealing RuvC for ssDNA access for *trans*-  
100 cleavage activity. Since we observe a slower *trans*-cleavage rate for longer fragments, we propose that  
101 steric hindrance by the staggered cut-end of the target DNA strand could induce a slower *trans*-  
102 cleavage activity. Shorter target lengths do not interfere with the RuvC catalytic site, and therefore  
103 enable direct *trans*-cleavage of ssDNA, without dependence on diffusive clearance or steric hindrance  
104 of the (remaining) *cis*-cleavage product. This also supports the observation that a decreased spacer  
105 length of the crRNA increases the *trans*-cleavage for both low GC containing and high GC containing  
106 sequences, which originates probably also from steric hindrance of the longer spacer sequence.

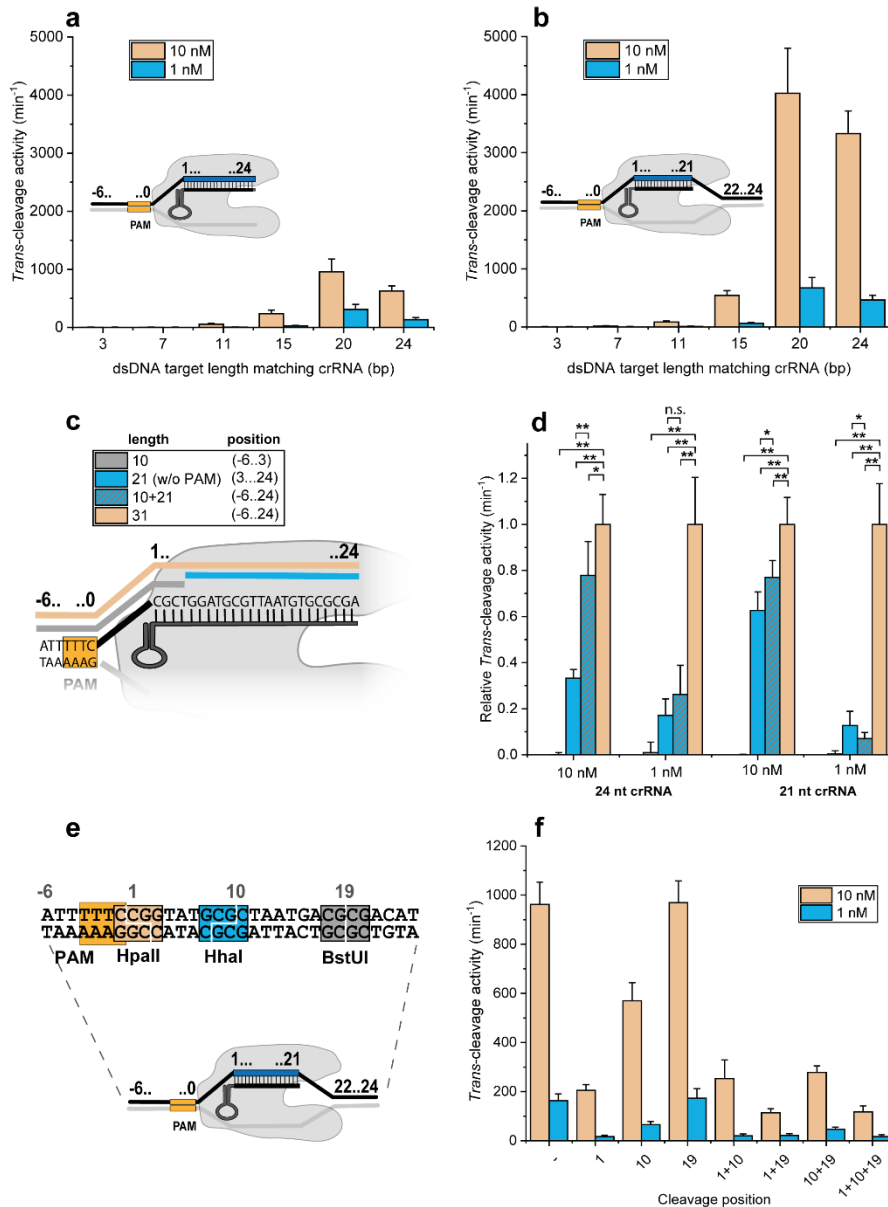


**Figure 1, Quantification of *trans*-cleavage activity using different dsDNA target fragments. High GC-content MAL sequence with a 3, 7, 11, 15, 20 and 24 bp target sequence that matches with a Cas12a ribonucleotide complex with a) a 24 nt crRNA spacer length and b) a 21 nt crRNA spacer length. c) Cartoon representation of Cas12a ribonucleotide complex with a 24 nt crRNA complex that binds to 10, 21, 10+21 and 31 bp fragments. d) Relative *trans*-cleavage rates of these different target lengths with the 24 and 21 nt spacer-crRNA. \*\* indicates  $p < 0.001$  and \* indicates  $p < 0.05$  (Two-sample T-test). e) Cartoon representation of the cleavage position of the MSREs on a 31 bp target sequence related to the crRNA. f) *Trans*-cleavage activity of a 31 bp total dsDNA target sequence, after treatment with a single type or a mixture of MSREs. In all figures error bars represent the mean  $\pm$  s.d., where  $n=9$  (three replicates for three independent targets).**

107 **Increased *trans*-cleavage in the presence of two fragments both complementing the crRNA spacer**  
108 Whereas experiments with different fragment lengths gave us some insight in the effect of shorter  
109 fragment lengths on the Cas12a *trans*-cleavage activity, utilizing MSREs will result in all fragments  
110 being present in the mixture in equimolar concentrations. In theory, this allows all fragments  
111 either individually or collectively to the crRNA. To mimic this situation, we carried out experiments  
112 with two fragments (21 bp and 10 bp) that together span the total 31 bp target sequence under the same  
113 experimental conditions as the fragmented targets (Figure 1c). Figure 1d shows the *trans*-cleavage  
114 activity of the different fragment lengths and the equimolar combination of the 10 and 21 bp  
115 fragments normalized to the *trans*-cleavage activity of 31 bp fragments at the same concentration.  
116 Remarkably, the activity resulting from 10 + 21 bp is in most conditions significantly higher than the  
117 sum of the activities for the individual 10 and 21 bp fragments ( $p < 0.05$ ), suggesting that both fragments  
118 can bind simultaneously to the crRNA, inducing a larger R-loop formation, resulting in higher *trans*-  
119 cleavage activity. The same trend was observed for low GC-content target sequences (Extended Data

120 Fig. 4), although the contribution of both fragments being present at equimolar concentrations was  
121 percentual less compared to high GC containing sequences. Additional experiments with high GC-  
122 content MAL sequences confirm that both fragments bind to the crRNA simultaneously (Extended Data  
123 Fig. 5). However, the simultaneous binding of both fragments decreases significantly at lower target  
124 DNA concentrations ( $p < 0.001$  for both crRNA lengths), which is observed as a relatively lower  
125 contribution of both fragments to the *trans*-cleavage activity for both high GC as low GC containing  
126 sequences.

127

### 128 **Trans-cleavage activity: cleavage position and fragment number matters**

129 We next tested whether the cleavage position on the target-DNA relatively to the PAM would affect  
130 the *trans*-cleavage activity. We designed a 31 bp dsDNA sequence with three MSRE recognition sites,  
131 which allowed us to selectively induce cleavage at different positions (Figure 1e). After overnight  
132 digestion with one single type or cocktails of MSREs, the Cas12a with associated crRNA was added and  
133 *trans*-cleavage was followed. Figure 1f shows the results of the *trans*-cleavage activity. PAM-proximal  
134 cleavage sites show the largest effect on the *trans*-cleavage activity, while PAM-distal cleavage at  
135 position 19 has no significant influence, which is in accordance with results discussed in previous  
136 work<sup>10,29-31</sup>. Combining cleavage sites decreases the relative *trans*-cleavage activity. This experiment  
137 gives crucial information for the crRNA design in single site CpG experiments, since the highest  
138 sensitivity is achieved for PAM-proximal non-methylated cytosines that are targeted by MSREs.

139

### 140 **Single CpG site methylation level quantification by combining MSREs and Cas12a sensing**

141 With the previous experiments we have confirmed that target DNA fragments without a PAM-proximal  
142 sequence result in a significantly lower *trans*-cleavage activity of Cas12a compared to sequences that  
143 match the entire crRNA sequence, or miss PAM-distal fragments even when both fragments are still  
144 present in the same solution. This opens the door for single CpG site methylation analysis, utilizing  
145 MSREs for fragmentation purposes. For these experiments, longer MAL gene DNA fragments of 120 bp  
146 were used to mimic a more realistic DNA fragment, as can typically be found in liquid biopsies like urine  
147 and blood<sup>32-34</sup>. We selected a crRNA that targets a single, PAM-proximal CpG site to achieve the highest  
148 sensitivity, as discussed in the previous section.

149

150 Figure 2a shows a schematic of the experimental outline for the detection of the methylation  
151 percentage of a single CpG site in the MAL gene. Since synthetic oligonucleotides are used in these  
152 experiments, methylation was performed with the M.SssI enzyme that, in principle, should methylate  
153 all CpGs of the oligonucleotide. Mock digestions were performed so that methylated and non-  
154 methylated DNA could be mixed in different ratios, to mimic different methylation percentages.  
155 Discrimination between methylated and non-methylated DNA is performed by Acil, which is a MSRE,  
156 with a recognition site that is PAM-proximal to the crRNA selected and results in two fragments that  
157 can be compared to the 10+21 bp fragments tested in the previous section. Using gel electrophoresis  
158 for fragmentation monitoring (Figure 2b), we observed some cleavage for the M.SssI-treated sample  
159 in the presence of Acil which suggests that either the M.SssI methylation was not complete, or Acil  
160 poses some non-specific activity resulting in underestimation of the methylation percentage. However,  
161 since we performed a calibration step this is not an issue for these experiments. Depending on the  
162 application and clinical setting of the assay one could optimize the MSRE digestion, resulting in either  
163 more false positives or false negatives.

164

165 After MSRE treatment, the different ratios methylated : non-methylated DNA were diluted to total  
166 DNA concentrations of 10, 5, 1 and 0.1 nM and added to Cas12a with a crRNA spacer length of either  
167 21 or 24 nt. Figure 2c shows the increase in fluorescence for the different ratios at a total DNA  
168 concentration of 10 nM with a crRNA length of 21 nt. The average slope of the linear section of these  
169 curves between 40 and 60 minutes was used to determine the average *trans*-cleavage activity. The  
170 effect of methylation on the *trans*-cleavage activity of Cas12a could be neglected, as this did not result  
171 in significant differences in average *trans*-cleavage activity (Extended Data Fig. 6). Figure 2d shows a  
172 linear fit with a  $R^2 = 0.999$  when plotting this *trans*-cleavage activity against the fraction of methylated  
173 DNA (for all other concentrations see extended Data Fig.7 for 21 nt crRNA-spacer). The slopes of the

174 curves corresponding to all different total DNA concentrations were plotted against the total DNA  
 175 concentration in Figure 2e, additionally showing the excellent sensitivity of Cas12a towards different  
 176 DNA concentrations. Utilizing 24 nt crRNA containing Cas12a resulted in similar linearity over both the  
 177 fraction methylated DNA and the total DNA concentration (extended Data Fig. 8).

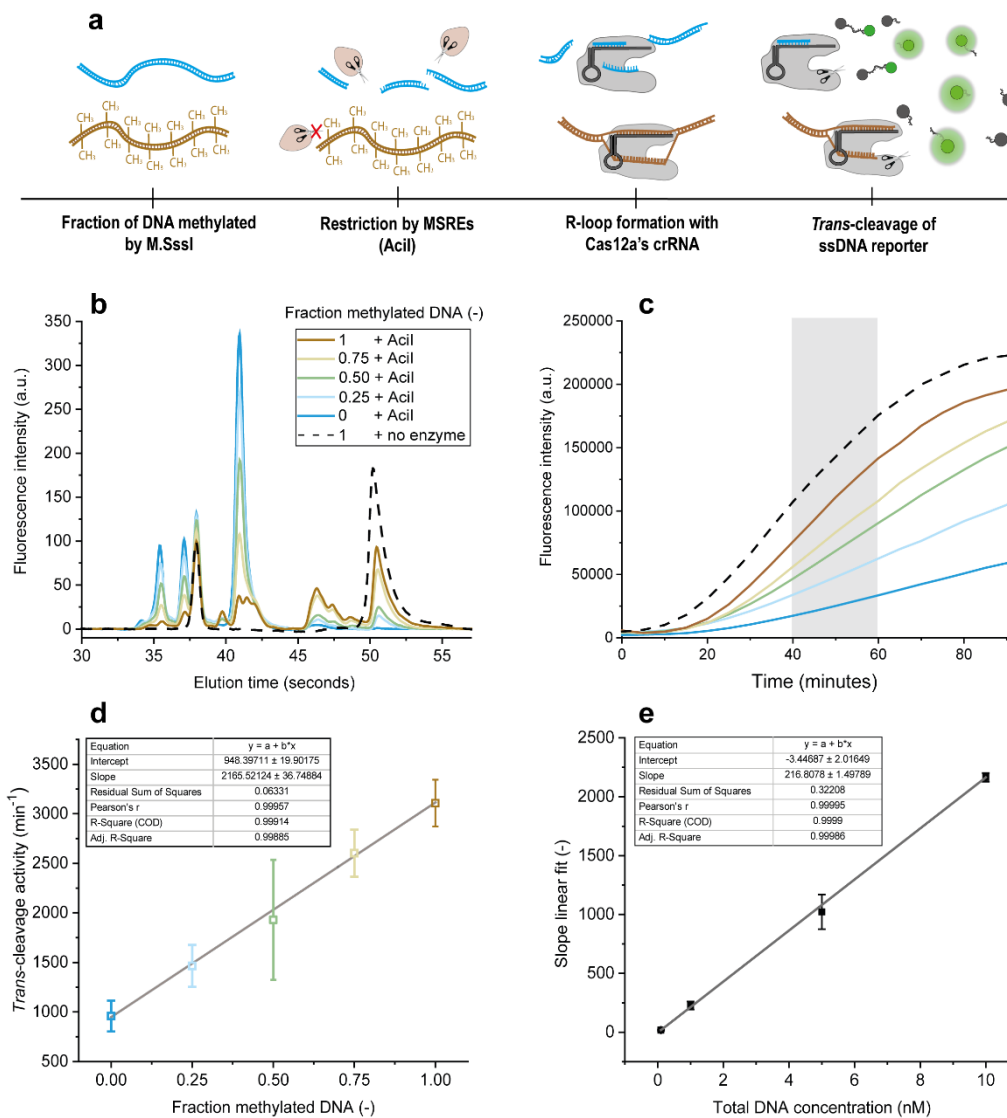


**Figure 2, a)** Schematic of time line for detection of methylation percentage of a single CpG site with MSREs and Cas12a. **b)** gel electrophoresis of methylated DNA without enzyme treatment and different fractions of methylated : non-methylated DNA after enzyme treatment. **c)** Increase in fluorescence over time for different fractions of methylated : non-methylated DNA after enzyme treatment at a total DNA concentration of 10 nM, in gray the time slot used for determination of the *trans*-cleavage activity. **d)** *Trans*-cleavage activity of different methylated DNA : non methylated DNA fraction at a total DNA concentration of 10 nM. Error bars represent the mean +/- s.d., where n=9 (three replicates for three independent targets). **e)** slope of the linear fit for the relation between fractions of methylated : non-methylated DNA against the *trans*-cleavage for different total DNA concentrations (0.1, 1, 5 and 10 nM). Error bars represent the mean +/- s.d. of the linear fit through the 5 data points per concentration.

## 178 Discussion

179 The methylation quantification method presented here for combined Cas12a–MSRE sensing opens the  
 180 possibility to identify individual CpG methylation sites in the genome by customizing the spacer  
 181 sequence, which is the section of the crRNA that hybridizes with the target DNA strand. The typical  
 182 length of this section of 20-24 nt offers the possibility of targeting unique sequences in most living  
 183 species. For example, in the human genome, 60% can be targeted as a unique sequence by customizing  
 184 the crRNA sequence<sup>35</sup>. Limitation of Cas12a is the PAM sequence, however, the world of biotechnology  
 185 is making great progress in the design of a PAM-free Cas nuclease, which will increase the possibilities  
 186 to target sequences tremendously<sup>36</sup>. Without the need of a PAM recognition sequence and the

187 information given in this paper the best possible crRNA-spacer sequences could be designed that offers  
188 the highest sensitivity for targeting single CpG sites in the entire genome.

189  
190 This new approach to epigenetic sequencing will allow extracting methylation patterns, providing as  
191 yet unknown patient data with the potential to revolutionize disease diagnostics. Furthermore,  
192 restriction enzymes can be exploited that can discriminate 5-methylcytosine (5-mC) from 5-  
193 hydroxymethylcytosine (5-hmC), which is one of the hot-topics in the epigenetics field<sup>37</sup>. The  
194 revolution in biotechnology also resulted in many manufactures providing ultra-fast enzymes that offer  
195 qualified digestion in 5-15 minutes. In combination with the relatively fast CRISPR/Cas12a based  
196 fluorescence detection (about 15 min - 1 hour depending on the input concentration), this method  
197 could easily be adapted to a point-of-care method, allowing quantitative and sensitive analysis in  
198 resource-poor settings<sup>38</sup>.

## 199 200 **Acknowledgements**

201 We would like to thank The Weijerhorst team from the University of Twente and the AmsterdamUMC  
202 for the fruitful collaboration. The Weijerhorst Foundation is acknowledged for their financial support.  
203

## 204 **References**

- 205 1. Chen, J. S. *et al.* CRISPR-Cas12a target binding unleashes indiscriminate single-stranded DNase  
206 activity. *Science (80-. )*. **360**, 436–439 (2018).
- 207 2. Abudayyeh, O. O. *et al.* C2c2 is a single-component programmable RNA-guided RNA-targeting  
208 CRISPR effector. *Science (80-. )*. **353**, aaf5573 (2016).
- 209 3. Anderson, E. M. *et al.* Systematic analysis of CRISPR-Cas9 mismatch tolerance reveals low levels  
210 of off-target activity. *J. Biotechnol.* **211**, 56–65 (2015).
- 211 4. Li, L. *et al.* HOLMESv2: A CRISPR-Cas12b-Assisted Platform for Nucleic Acid Detection and DNA  
212 Methylation Quantitation. *ACS Synth. Biol.* **8**, 2228–2237 (2019).
- 213 5. Gootenberg, J. S. *et al.* Nucleic acid detection with CRISPR-Cas13a/C2c2. *Science (80-. )*. **356**,  
214 438–442 (2017).
- 215 6. Adli, M. The CRISPR tool kit for genome editing and beyond. *Nat. Commun.* **9**, (2018).
- 216 7. Terns, M. P. CRISPR-Based Technologies: Impact of RNA-Targeting Systems. *Molecular Cell* **72**,  
217 404–412 (2018).
- 218 8. Manghwar, H., Lindsey, K., Zhang, X. & Jin, S. CRISPR/Cas System: Recent Advances and Future  
219 Prospects for Genome Editing. *Trends Plant Sci.* **24**, 1102–1125 (2019).
- 220 9. Zhang, S. *et al.* Recent Advances of CRISPR/Cas9-Based Genetic Engineering and Transcriptional  
221 Regulation in Industrial Biology. *Front. Bioeng. Biotechnol.* **7**, 1–11 (2020).
- 222 10. Strohkendl, I., Saifuddin, F. A., Rybarski, J. R., Finkelstein, I. J. & Russell, R. Kinetic Basis for DNA  
223 Target Specificity of CRISPR-Cas12a. *Mol. Cell* **71**, 816-824.e3 (2018).
- 224 11. Jinek, M. *et al.* A programmable dual-RNA-guided DNA endonuclease in adaptive bacterial  
225 immunity. *Science (80-. )*. **337**, 816–821 (2012).
- 226 12. Jeon, Y. *et al.* Direct observation of DNA target searching and cleavage by CRISPR-Cas12a. *Nat.*  
227 *Commun.* **9**, (2018).
- 228 13. Calzone, K. A. Genetic Biomarkers of Cancer Risk. *Semin. Oncol. Nurs.* **28**, 122–128 (2012).
- 229 14. Robertson, K. D. DNA methylation and human disease. *Nature Reviews Genetics* **6**, 597–610  
230 (2005).

- 231 15. Bosschieter, J. *et al.* A protocol for urine collection and storage prior to DNA methylation  
232 analysis. *PLoS One* **13**, e0200906 (2018).
- 233 16. Steenbergen, R. D. M. *et al.* TSLC1 gene silencing in cervical cancer cell lines and cervical  
234 neoplasia. *J. Natl. Cancer Inst.* **96**, 294–305 (2004).
- 235 17. Warnecke, P. M. *et al.* Identification and resolution of artifacts in bisulfite sequencing. *Methods*  
236 **27**, 101–107 (2002).
- 237 18. Šestáková, Š., Šálek, C. & Remešová, H. DNA Methylation Validation Methods: A Coherent  
238 Review with Practical Comparison. *Biological Procedures Online* **21**, 19 (2019).
- 239 19. Zou, B. *et al.* Correlation Between the Single-Site CpG Methylation and Expression Silencing of  
240 the XAF1 Gene in Human Gastric and Colon Cancers. *Gastroenterology* **131**, 1835–1843 (2006).
- 241 20. Sohn, B. H. *et al.* Functional Switching of TGF- $\beta$ 1 Signaling in Liver Cancer via Epigenetic  
242 Modulation of a Single CpG Site in TTP Promoter. *Gastroenterology* **138**, 1898-1908.e12 (2010).
- 243 21. Swarts, D. C., van der Oost, J. & Jinek, M. Structural Basis for Guide RNA Processing and Seed-  
244 Dependent DNA Targeting by CRISPR-Cas12a. *Mol. Cell* **66**, 221-233.e4 (2017).
- 245 22. Lind, G. E. *et al.* Hypermethylated MAL gene - A silent marker of early colon tumorigenesis. *J.*  
246 *Transl. Med.* **6**, 13 (2008).
- 247 23. Choi, B. *et al.* MAL and TMEM220 are novel DNA methylation markers in human gastric cancer.  
248 *Biomarkers* **22**, 35–44 (2017).
- 249 24. Overmeer, R. M. *et al.* Repression of MAL tumour suppressor activity by promoter methylation  
250 during cervical carcinogenesis. *J. Pathol.* **219**, 327–336 (2009).
- 251 25. Buffart, T. E. *et al.* MAL promoter hypermethylation as a novel prognostic marker in gastric  
252 cancer. *Br. J. Cancer* **99**, 1802–1807 (2008).
- 253 26. Bosschieter, J. *et al.* A two-gene methylation signature for the diagnosis of bladder cancer in  
254 urine. *Epigenomics* **11**, 337–347 (2019).
- 255 27. Nguyen, L. T., Smith, B. M. & Jain, P. K. Enhancement of trans-cleavage activity of Cas12a with  
256 engineered crRNA enables amplified nucleic acid detection. *Nat. Commun.* **11**, 1–13 (2020).
- 257 28. Fuchs, R. T., Curcuru, J., Mabuchi, M., Yourik, P. & Robb, G. B. Cas12a trans-cleavage can be  
258 modulated in vitro and is active on ssDNA, dsDNA, and RNA. *bioRxiv* 600890 (2019).  
259 doi:10.1101/600890
- 260 29. Swarts, D. C., van der Oost, J. & Jinek, M. Structural Basis for Guide RNA Processing and Seed-  
261 Dependent DNA Targeting by CRISPR-Cas12a. *Mol. Cell* **66**, 221-233.e4 (2017).
- 262 30. Yamano, T. *et al.* Crystal Structure of Cpf1 in Complex with Guide RNA and Target DNA. *Cell* **165**,  
263 949–962 (2016).
- 264 31. Gao, P., Yang, H., Rajashankar, K. R., Huang, Z. & Patel, D. J. Type v CRISPR-Cas Cpf1  
265 endonuclease employs a unique mechanism for crRNA-mediated target DNA recognition. *Cell*  
266 *Res.* **26**, 901–913 (2016).
- 267 32. Liu, X. *et al.* Fragment Enrichment of Circulating Tumor DNA With Low-Frequency Mutations.  
268 *Front. Genet.* **11**, (2020).
- 269 33. Underhill, H. R. *et al.* Fragment Length of Circulating Tumor DNA. *PLOS Genet.* **12**, e1006162  
270 (2016).
- 271 34. Alcaide, M. *et al.* Evaluating the quantity, quality and size distribution of cell-free DNA by  
272 multiplex droplet digital PCR. *Sci. Rep.* **10**, 12564 (2020).

- 273 35. Misawa, K. Distribution of unique sequences in the human genome. *Austin J Comput Biol*  
274 *Bioinform.* **2**, 1010 (2015).
- 275 36. Collias, D. & Beisel, C. L. CRISPR technologies and the search for the PAM-free nuclease. *Nature*  
276 *Communications* **12**, 1–12 (2021).
- 277 37. Branco, M. R., Ficz, G. & Reik, W. Uncovering the role of 5-hydroxymethylcytosine in the  
278 epigenome. *Nat. Rev. Genet.* **13**, 7–13 (2012).
- 279 38. van Dongen, J. E. *et al.* Point-of-care CRISPR/Cas nucleic acid detection: Recent advances,  
280 challenges and opportunities. *Biosens. Bioelectron.* **166**, 112445 (2020).
- 281